Calibrating the energy of a 50×50 GeV muon collider using spin precession

Rajendran Raja and Alvin Tollestrup
Fermi National Accelerator Laboratory, P.O. Box 500, Batavia, Illinois 60510
(Received 6 January 1998; published 19 May 1998)

The neutral Higgs boson is expected to have a mass in the region 90–150 GeV/c^2 in various schemes within the minimal supersymmetric extension of the standard model. A first generation muon collider is uniquely suited to investigate the mass, width, and decay modes of the Higgs boson, since the coupling of the Higgs boson to muons is expected to be strong enough for it to be produced in the *s* channel mode in the muon collider. Because of the narrow width of the Higgs boson, it is necessary to measure and control the energy of the individual muon bunches to a precision of a few parts in a million. We investigate the feasibility of determining the energy scale of a muon collider ring with circulating muon beams of 50 GeV energy by measuring the turn by turn variation of the energy deposited by electrons produced by the decay of the muons. This variation is caused by the existence of an average initial polarization of the muon beam and a nonzero value of $g-2$ for the muon. We demonstrate that it is feasible to determine the energy scale of the machine with this method to a few parts per million using data collected during 1000 turns. [S0556-2821(98)02213-9]

PACS number(s): 14.80.Bn, 13.10.+q

I. METHOD

The spin vector $\vec{S}$ of a muon in the muon collider will precess according to the following equation, first derived by Bargmann, Michel, and Telegdi [1]:

$$\frac{d\vec{S}}{dt}=\vec{\Omega}\times\vec{S}, \tag{1.1}$$

$$\vec{\Omega}=-\frac{e}{\gamma m_\mu}\left[(1+a\gamma)\vec{B}_\perp+(1+a)\vec{B}_\parallel-\left(a\gamma+\frac{\gamma}{1+\gamma}\right)\vec{\beta}\times\frac{\vec{E}}{c}\right], \tag{1.2}$$

where $\vec{B}_\perp$ and $\vec{B}_\parallel$ are the transverse and parallel components of the magnetic field with respect to the muon's velocity $\vec{\beta}c$, e is the electric charge, m_μ the mass of the muon, $a\equiv(g-2)/2$ is the magnetic moment anomaly of the muon, and γ and g are the Lorentz factor and the gyromagnetic ratio of the muon. The value of $a\equiv(g-2)/2$ for the muon is $1.165\,924\times10^{-3}$ [2]. In what follows, we will consider the ideal planar collider ring case where $\vec{B}_\parallel$ and $\vec{E}$ are zero. For such a collider ring, $\vec{\Omega}$ is given by

$$\vec{\Omega}=\vec{\Omega}_{cyc}(1+a\gamma), \tag{1.3}$$

where $\vec{\Omega}_{cyc}$ is the angular velocity of the circulating beam. From this, it follows that when the beam completes one turn, the spin will rotate by a further $a\gamma\times2\pi$ rad. We will compute the precision with which γ can be determined by measuring the energy of the electrons produced by muon decay in this ideal case. We will examine the effects of departures from the ideal case in the last section.

It can be shown that the angular distribution of the decay electrons in the muon center of mass is given by the relation [3]

$$\frac{d^2N}{dx\,d\cos\theta}=N[x^2(3-2x)-\hat{P}x^2(1-2x)\cos\theta], \tag{1.4}$$

where N denotes the number of muon decays, $x\equiv2E/m_\mu$ is the electron energy E in the muon rest frame expressed as a fraction of the maximum possible energy ($\approx0.5m_\mu$), $\cos\theta$ is the angle of the electron in the muon rest frame with respect to the z axis which is the direction of motion of the muon in the laboratory, and $\hat{P}$ is the product of the muon charge and the z component of the muon polarization. The muon polarization is defined as the average of the individual muon unit spin vectors over the ensemble of muons considered. We note that the distribution is linear in $\hat{P}$.

A routine was written to generate muon decays according to Eq. (1.4). Figure 1 shows the shape of the function in Eq. (1.4) and the generated events in $x,\cos\theta$ space for various values of $\hat{P}$. There is excellent agreement between the theoretical shape of the function and the Monte Carlo–generated events. The average energy $\langle E\rangle$ and longitudinal momentum $\langle P_L\rangle$ of the electron in the muon rest frame can be obtained using Eq. (1.4) as follows:

$$\langle E\rangle=\frac{m_\mu}{2}\int\int x\frac{d^2N}{dx\,d\cos\theta}dx\,d\cos\theta=\frac{7}{10}\frac{m_\mu}{2}, \tag{1.5}$$

$$\langle P_L\rangle=\frac{m_\mu}{2}\int\int x\cos\theta\frac{d^2N}{dx\,d\cos\theta}dx\,d\cos\theta=\frac{\hat{P}}{10}\frac{m_\mu}{2}. \tag{1.6}$$

These two quantities form the components of a four-vector, whose transverse components are zero, which may be transformed to the laboratory frame to yield the average electron energy $\langle E_{lab}\rangle$:

$$\langle E_{lab}\rangle=\frac{7}{20}E_\mu\left(1+\frac{\beta}{7}\hat{P}\right), \tag{1.7}$$

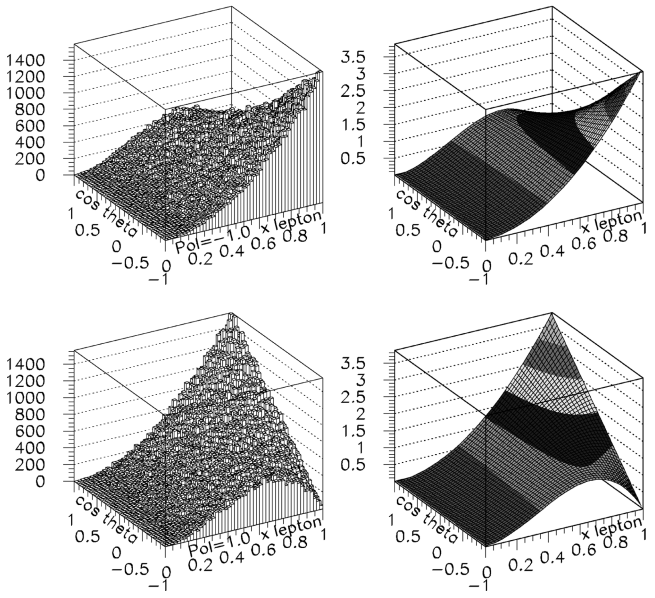

FIG. 1. The top lego plots show the generated events and the theoretical decay function in the $x,\cos\theta$ plane for $\hat{P}=-1.0$. The lego plots at the bottom of the figure show the corresponding plots for $\hat{P}=1.0$.

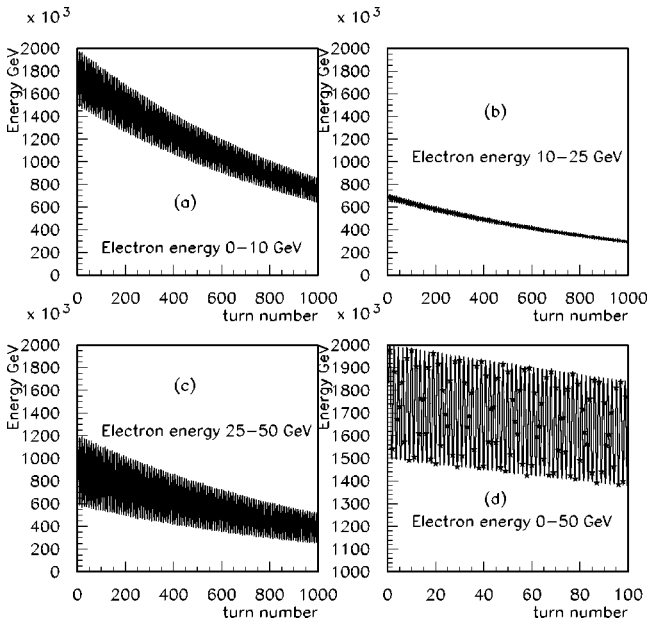

FIG. 2. (a)Total energy observed as a function of turn number for $\hat{P}=-1.0$ with individual electron energies in the range 0–10 GeV for 100 000 muon decays. Electron energies in the range (b) 10–25 GeV and (c) 25–50 GeV. (d) All electrons included. Superimposed is a functional form defined by Eq. (1.8).

where E_μ is the energy of the muon beam. Since the polarization $\hat{P}$ precesses from turn to turn by the amount $\omega=\gamma(g-2)/2\times 2\pi$ rad and the number of muons decreases turn by turn due to decay and losses, the total energy $E(t)$ due to decay electrons observed during turn t in an electromagnetic calorimeter will have the following expression:

$$E(t)=Ne^{(-\alpha t)}\left[\frac{7}{20}E_\mu\left(1+\frac{\beta}{7}(\hat{P}\cos\omega t+\phi)\right)\right], \quad (1.8)$$

where N is the number of muon decays sampled in turn 0, ϕ is an arbitrary phase containing information on the initial direction of polarization, and α is the turn-by-turn decay constant of the muon intensity which in the absence of losses other than decay is given by

$$\alpha=\frac{t_{circ}}{\gamma t_{life}}, \quad (1.9)$$

where t_{circ} is the time taken to circulate around the storage ring and t_{life} is the muon lifetime.

For a 100% polarized beam, the amplitude of the oscillations is only 1/7 that of the nonoscillating background. It can be seen from Eq. (1.4) that the sensitivity to $\hat{P}$ is enhanced by selecting larger values of $\cos\theta$. This implies selecting electrons with higher laboratory energy. Figures 2(a)–2(c) show the deposited electron energy as a function of turn number for polarization $\hat{P}=1.0$ for individual electron energy ranges of 0–10 GeV, 10–25 GeV, and 25–50 GeV, respectively, as a function of turn number. Figure 2(b) shows very little oscillatory signal, since the electrons in that energy range have small values of $\cos\theta$. Figure 2(d) shows the deposited electron energy with no electron energy cuts. Superimposed is the predicted behavior according to Eq. (1.8). This serves as a consistency check for our routines. The signal-to-background ratio increases as we demand electrons with higher values of $\cos\theta$. In what follows, we use electrons with energy greater than 25 GeV during the investigative phase of this analysis and will later optimize this cut. In practice, we can select electrons with energies above a value by momentum analyzing them with a dipole field before they enter the calorimeter.

The method to determine the energy scale of the collider would then entail fitting a functional form of the type

$$f(t)=Ae^{-Bt}[C\cos(D+Et)+F] \quad (1.10)$$

to the energy observed in the calorimeter. The variables A,B,C,D,E,F are parameters to be fitted. The information on the energy scale is contained in the parameter E.

A. Parameters of a 50 GeV idealized muon storage ring

In order to arrive at reasonable numbers for α and ω, we consider a storage ring of 50 GeV muons with a uniform bending field of 4 T. This would produce a circular ring with the parameters given in Table I. It should be noted that for an idealized storage ring with constant B field considered here, α does not depend on γ, since

$$t_{circ}=\frac{m_\mu\gamma}{0.3Bc}, \quad (1.11)$$

$$\alpha=\frac{2\pi m_\mu}{0.3Bct_{life}}, \quad (1.12)$$

TABLE I. Parameters of an idealized muon storage ring.

Parameter	Value	Parameter	Value
Muon energy	50 GeV	γ	473.22
Spin precession in one turn	3.4667 rad	Magnetic field	4.0 T
Radius of ring	41.666 66 m	Beam circulation time	$0.873\,27\times10^{-6}$ sec
Dilated muon lifetime	$0.103\,97\times10^{-2}$ sec	Turn-by-turn decay constant	0.8399×10^{-3}

where m_μ is the muon rest mass, B is the bending field of the storage ring, and c is the velocity of light. A 100 GeV collider ring will have the same α as a 50 GeV collider ring or a 25 GeV collider ring in this idealized case. As γ changes slightly, t_{circ} changes in proportion, α being the constant used to convert measurements of t_{circ} to γ. Measuring the decay rate of muons also affords a second method to determine γ. The beam circulation time t_{circ} can be measured to precisions of the order of 1 part in 10^6 and the fractional error in the muon lifetime is 1.82×10^{-5} [2]. The fractional error in γ obtainable by observing the rate of decay of the muons will then be dominated by the precision that one can measure α, namely, $\delta\gamma/\gamma=\delta\alpha/\alpha$.

B. Generation of events and fitting for γ

Since Eq. (1.4) is linear in $\hat{P}$, the decay distribution of an ensemble of muons depends only on $\hat{P}$, the ensemble average of the z component of the individual muon spin vectors. However, because of the momentum spread of the muons, each individual particle will have a γ slightly different from the average and hence the precession of the spin vector around the ring will be different, leading to a slightly different value of $\hat{P}$ for the next turn. We model the beam by generating an ensemble of 100 000 muons, each having its own spin vector and momentum. In an actual collider, it will be possible to sample significantly more decays than this. During each turn, we decay all the beam particles once and record the number and total energy deposited by electrons with individual energies above 25 GeV. Approximately 27% of the decay electrons pass this cut, on average. We decrease the number of decays by the appropriate number expected by muon decay alone for the next turn. At this stage we do not introduce fluctuations in the number of decays from turn to turn, since the 100 000 muons are meant to be representative of a much larger number in the actual ring. We precess the 100 000 spin vectors by their individual precession rates and make them decay again. We repeat this for 1000 turns. We reuse the muons after each turn since the 100 000 muons represent our model of the muon ensemble in the collider.

1. Generation of muon spin vectors

We generate four different samples of events with different ensembles of spin vectors. The z component of the unit spin vector of a muon S_z is allowed to vary from -1 to 1. This range is divided into 51 bins and the z components are generated using a binomial distribution whose average value is specified. We are justified in treating this problem in this classical fashion, since each ''muon'' represents an ensemble of actual muons with quantized spin components. A more realistic generation of the spin vectors with correlations between momentum spread and $\hat{P}$ would require a detailed modelling of the pion decay and muon transport systems and is not warranted here since the effect due to the distribution in S_z is expected to be small. Figures 3(a)–3(d) show the distributions of S_z for the four samples. The average values of the distributions are 0.9, 0.74, 0.5, and 0.26, respectively. We study negatively charged muons resulting in an initial value of $\hat{P}$ of -0.9, -0.74, -0.5, and -0.26, respectively, for these samples. In the absence of momentum spread, the decay distributions would only depend on $\hat{P}$ and not on the details of the distribution of S_z. The angles of the spin vectors are precessed by the individual γ-dependent precession rate from turn to turn. In what follows, we assume a beam energy spread of 0.03% for the muons for all samples unless otherwise specified.

2. Fitting procedure and generation of errors

The energy deposited every turn is fitted to the functional form given by Eq. (1.10) using the CERN program MINUIT [4]. In order to study the variation of the fractional error $\delta\gamma/\gamma$ with the number of electrons sampled, we fluctuate the energy observed in the calorimeter E_m by

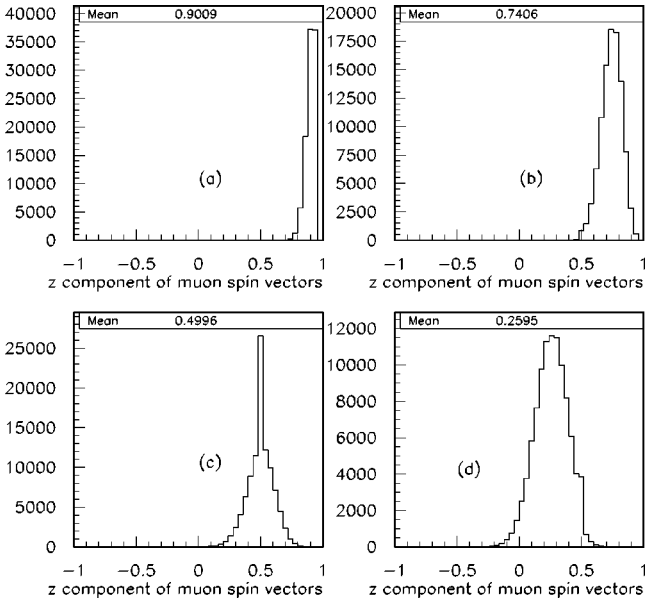

FIG. 3. (a)–(d) show the distribution of the z component of the spin vectors for the four samples considered.

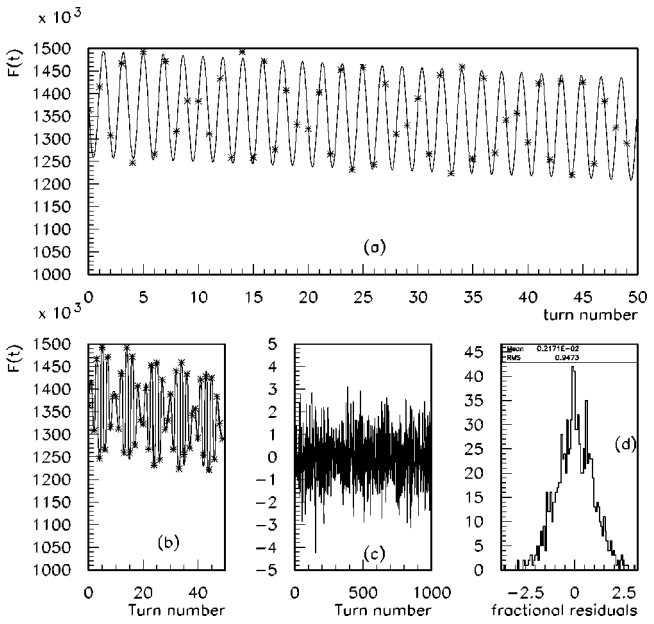

FIG. 4. (a) Energy detected in the calorimeter during the first 50 turns in a 50 GeV muon storage ring (points). An average value of $\hat{P}=-0.26$ is assumed and a fractional fluctuation of 0.5×10^{-2} per point. The curve is the result of a MINUIT fit to the functional form in Eq. (1.10). (b) The same fit, with the function being plotted only at integer turn values. A beat is evident. (c) Pulls as a function of turn number. (d) Histogram of pulls.

$$\frac{\sigma_{E_m}^2}{\langle E_m\rangle^2}\approx\frac{1}{N}(1.03153), \tag{1.13}$$

where N is the number of electrons sampled. See the Appendix for a derivation of this formula. We analyze the case for 41 261, 10 315, 2579, and 1146 electrons sampled which corresponds to a fractional error in the measured total energy of PERR $\equiv\sigma_{E_m}/E_m$ of 0.5×10^{-2}, 1.0×10^{-2}, 2.0×10^{-2}, and 3.0×10^{-2}, respectively.

II. RESULTS

We simulate the muon collider spin precession for a grid of values of $\hat{P}=-0.9$, -0.74, -0.5, and -0.26 and fractional measurement error for the first turn (PERR) of 0.5×10^{-2}, 1.0×10^{-2}, 2.0×10^{-2}, and 3.0×10^{-2}. Figure 4(a) shows the result of the MINUIT fit plotted for 50 turns for $\hat{P}=-0.26$ and PERR$=0.5\times10^{-2}$. Figure 4(b) shows the same plot but with the function being plotted only at integer values of the turn number t. A beat is evident in both the theoretical curve and the simulated measurements as a result of sampling the oscillation function at fixed intervals, not connected with the oscillation frequency. The origin of the beat is stroboscopic. Figure 4(c) shows the pulls, defined as (data-fit)/error at each measurement as a function of turn number for 1000 turns. There are no major turn-dependent variations in this quantity, indicating that the fit converged satisfactorily. Figure 4(d) shows the histogram of the pulls, which approximates a unit Gaussian as desired. Table II shows the results of the fit for the grid of values of $\hat{P}$ and PERR. The results presented in Table II are shown graphically in Fig. 5. As an example, for an average polarization $\hat{P}=-0.26$, the fractional error in $\delta\gamma/\gamma$ varies from 5.1×10^{-6} to 1.9×10^{-5} as the fractional error in the electron energy sampled varies from 0.5×10^{-2} to 3.0×10^{-2}, corresponding to the number of electrons sampled during the first turn varying from 41 261 to 1146. The average number of decays in the muon collider is expected to be 3.2×10^{6} de-

TABLE II. Results of fits for $\delta\gamma/\gamma$ as a function of polarization $\hat{P}$ and noise PERR. Also shown is the χ^2 of the fit for 1000 turns.

$\hat{P}$	PERR	Number of electrons sampled	$\delta\gamma/\gamma$ oscillations	$\delta\gamma/\gamma$ decay	χ^2 for $N_{\rm DF}=1000$
-0.90	0.50×10^{-2}	41 261	$0.145\,68\times10^{-5}$	$0.132\,27\times10^{-2}$	824
-0.90	0.10×10^{-1}	10 315	$0.221\,47\times10^{-5}$	$0.201\,24\times10^{-2}$	936
-0.90	0.20×10^{-1}	2579	$0.399\,99\times10^{-5}$	$0.363\,98\times10^{-2}$	1009
-0.90	0.30×10^{-1}	1146	$0.586\,59\times10^{-5}$	$0.534\,57\times10^{-2}$	1030
-0.74	0.50×10^{-2}	41 261	$0.174\,18\times10^{-5}$	$0.130\,19\times10^{-2}$	843
-0.74	0.10×10^{-1}	10 315	$0.261\,83\times10^{-5}$	$0.195\,91\times10^{-2}$	954
-0.74	0.20×10^{-1}	2579	$0.469\,81\times10^{-5}$	$0.352\,29\times10^{-2}$	1021
-0.74	0.30×10^{-1}	1146	$0.687\,65\times10^{-5}$	$0.516\,72\times10^{-2}$	1039
-0.50	0.50×10^{-2}	41 261	$0.259\,03\times10^{-5}$	$0.128\,13\times10^{-2}$	888
-0.50	0.10×10^{-1}	10 315	$0.384\,07\times10^{-5}$	$0.190\,29\times10^{-2}$	973
-0.50	0.20×10^{-1}	2579	$0.683\,38\times10^{-5}$	$0.339\,72\times10^{-2}$	1026
-0.50	0.30×10^{-1}	1146	$0.997\,44\times10^{-5}$	$0.497\,49\times10^{-2}$	1041
-0.26	0.50×10^{-2}	41 261	$0.512\,42\times10^{-5}$	$0.126\,88\times10^{-2}$	898
-0.26	0.10×10^{-1}	10 315	$0.753\,17\times10^{-5}$	$0.187\,91\times10^{-2}$	1004
-0.26	0.20×10^{-1}	2579	$0.133\,24\times10^{-4}$	$0.334\,47\times10^{-2}$	1053
-0.26	0.30×10^{-1}	1146	$0.193\,80\times10^{-4}$	$0.489\,50\times10^{-2}$	1061

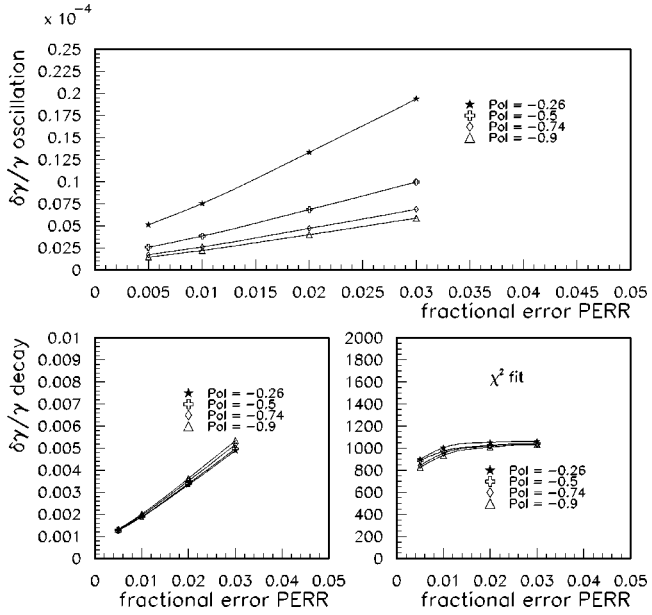

FIG. 5. (a) Fractional error in $\delta\gamma/\gamma$ obtained from the oscillations as a function of polarization $\hat{P}$ and the fractional error in the measurements PERR. (b) Fractional error in $\delta\gamma/\gamma$ obtained from the decay term as a function of polarization $\hat{P}$ and the fractional error in the measurements PERR. (c) The total χ^2 of the fits for 1000 degrees of freedom.

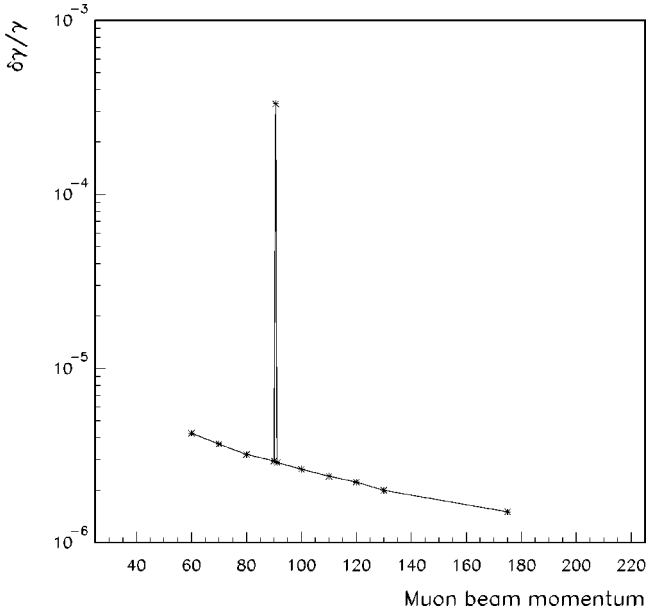

FIG. 6. Fractional error in $\delta\gamma/\gamma$ obtained from the oscillations as a function of muon beam momentum.

cays per meter for a beam intensity of 10^{12} muons. The error in determining γ is thus going to be dominated by the fluctuations in the number of electrons sampled turn by turn, rather than sampling fluctuations in the calorimeter. We have simulated conditions involving $\approx$40 000 decays. It should be possible to go to higher statistical precision than computed here by sampling a larger number of electrons.

The results for $\delta\gamma/\gamma$ obtained from the measurement of the turn-by-turn rate of decay of the electron energy are not competitive with the precession method primarily because of the small value of α (0.8399×10^{-3}). This leads to larger fractional errors for γ from this method (which also assumes that the loss of intensity is entirely due to the decay process) by almost three orders of magnitude than from the precession method.

A. Variation of $\delta\gamma/\gamma$ as a function of muon energy

The spin precession per turn equals 2π for a γ value of 857.689, which corresponds to a muon beam momentum of 90.622 GeV/c. This is the first spin resonance for muons. At this point, the fitting method loses sensitivity completely, since there will be no spin oscillations turn by turn. We now study the error $\delta\gamma/\gamma$ as a function of beam energy for $\hat{P}=-0.26$ and PERR$=0.5\times10^{-2}$ (keeping the magnetic field in the idealized storage ring to be 4.0 T) as a function of muon beam energy that straddles the spin resonance. For initial muon collider physics, the interesting beam energies are 45.5 GeV (half the Z mass), 80.3 GeV (W threshold), and 175 GeV (top threshold) as well as half the neutral Higgs boson mass, which could be as low as 55 GeV in some supersymmetry (SUSY) scenarios. We sample all electrons that have energies greater than half the muon energy. Figure 6 shows the variation of $\delta\gamma/\gamma$ as a function of muon beam energies that straddle these values. It can be seen that $\delta\gamma/\gamma$ first decreases as one gets close to the resonance and then blows up on the spin resonance. Figures 7–12 show the fitted solutions superimposed on the simulated data for various momenta. Also shown side by side is the simulated data by

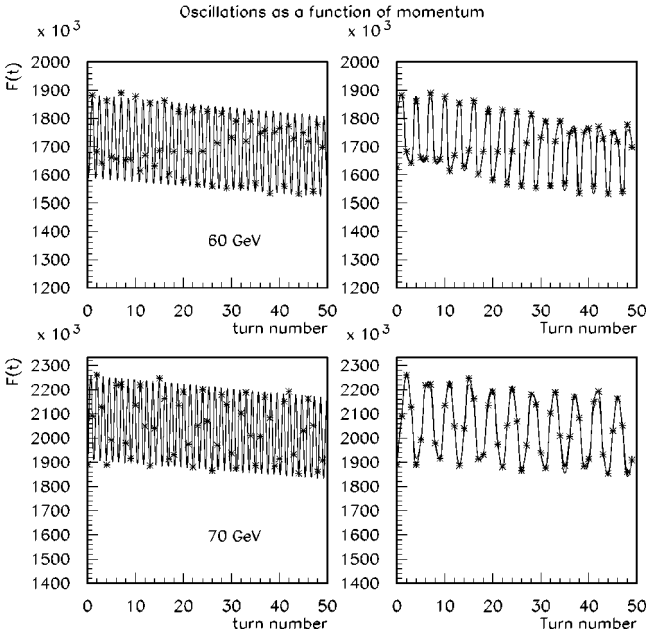

FIG. 7. The figures on the left hand side show the simulated data with the fitted function superimposed for 50 turns. The figures on the right hand side show the simulated data and the fitted function at integer values of the turn number. The data shown are 60 GeV/c and 70 GeV/c muon momenta, respectively.

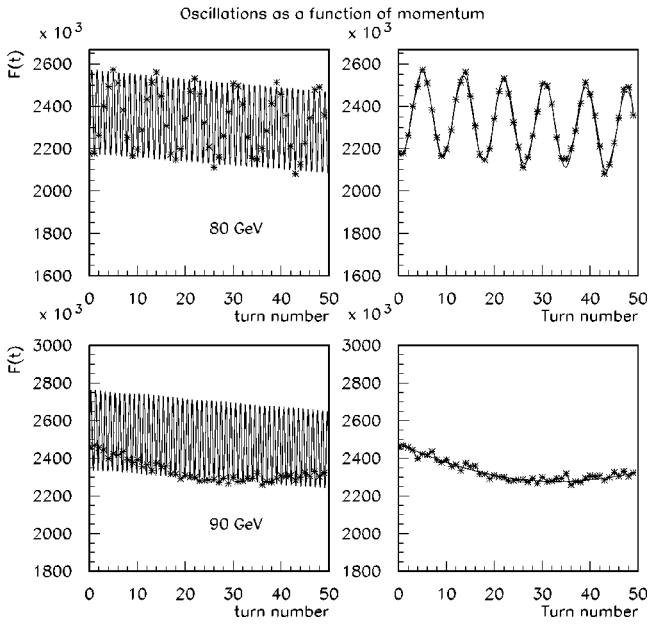

FIG. 8. The figures on the left hand side show the simulated data with the fitted function superimposed for 50 turns. The figures on the right hand side show the simulated data and the fitted function at integer values of the turn number. The data shown are 80 GeV/c and 90 GeV/c muon momenta, respectively.

itself. As one approaches the spin resonance, the oscillations slow down. It is nevertheless possible to fit the slowed down oscillations by a rapidly oscillating theoretical function to high accuracy on either side of the resonance. At the resonance, the oscillations die completely, which results in a large value of $\delta\gamma/\gamma$. It may be possible to use this blowup in $\delta\gamma/\gamma$ to find the spin resonance accurately and (paradoxically) determine γ at resonance accurately. This would depend on the width of the spin resonance, an analysis of which would take us beyond the scope of this paper.

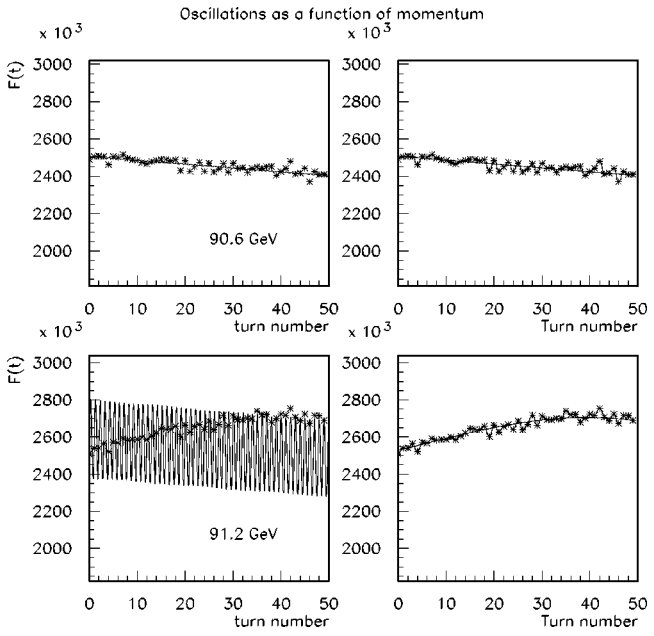

FIG. 9. The figures on the left hand side show the simulated data with the fitted function superimposed for 50 turns. The figures on the right hand side show the simulated data and the fitted function at integer values of the turn number. The data shown are 90.622 GeV/c and 91.2 GeV/c muon momenta, respectively. The upper curve is on resonance.

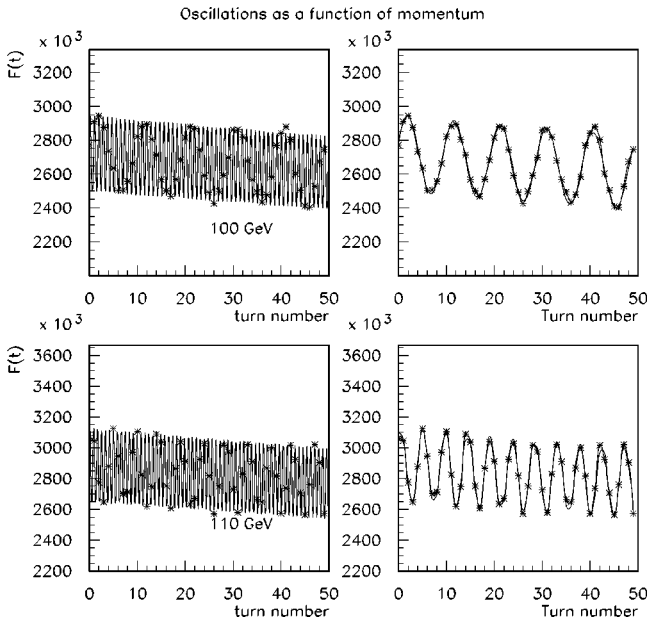

FIG. 10. The figures on the left hand side show the simulated data with the fitted function superimposed for 50 turns. The figures on the right hand side show the simulated data and the fitted function at integer values of the turn number. The data shown are 100 GeV/c and 110 GeV/c muon momenta, respectively.

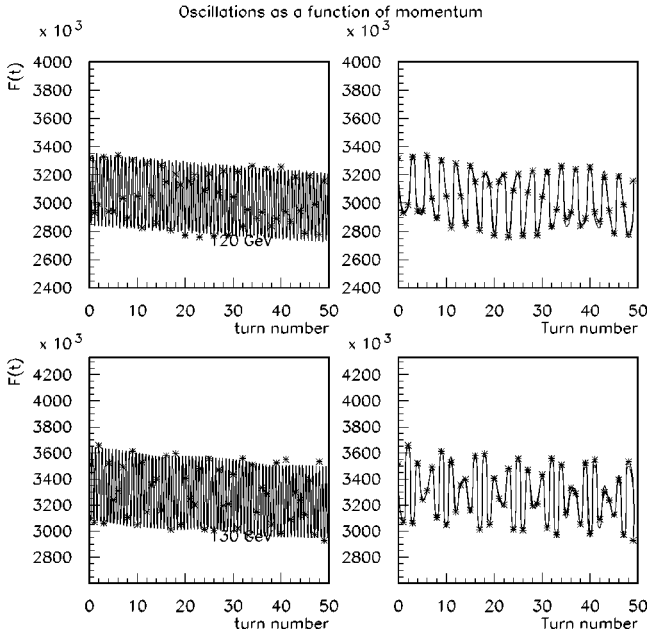

FIG. 11. The figures on the left hand side show the simulated data with the fitted function superimposed for 50 turns. The figures on the right hand side show the simulated data and the fitted function at integer values of the turn number. The data shown are 120 GeV/c and 130 GeV/c muon momenta, respectively.

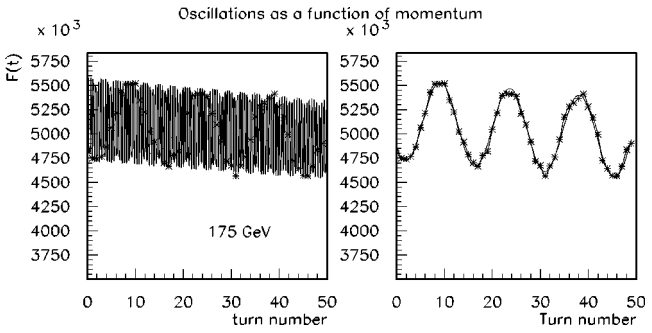

FIG. 12. The figure on the left hand side show the simulated data with the fitted function superimposed for 50 turns. The figure on the right hand side show the simulated data and the fitted function at integer values of the turn number. The data shown are 175 GeV/c muon momentum.

B. Variation of $\delta\gamma/\gamma$ as a function of beam energy spread

We now calculate the variation of polarization as a function of turn number for an ensemble of muons with initial value of polarization $\hat{P}=-0.26$ and values of the momentum spread $\delta p/p$ varying from 0.02×10^{-2} to 0.00125×10^{-2}. This variation is plotted in Fig. 13. For the larger values of the momentum spread, there is a significant degradation of polarization as a function of turn number, due to the differential spin precession of the individual beam particles. We note that when the beam energy is at 175 GeV, the spin tune is significantly higher and the depolarization is more rapid. Despite this depolarization, there is enough information from the first few hundred turns to extract the excellent value of $\delta\gamma/\gamma$ for 175 GeV beam energy as shown in Fig. 6.

Figure 14 shows the variation of the fractional energy resolution, $\delta\gamma/\gamma$, as a function of fractional beam energy spread for a muon beam with $\hat{P}=-0.26$, with 41 261 electrons sampled. There is little dependence of $\delta\gamma/\gamma$ on the momentum spread. This is due to the fact that the momentum spread is determined from the spin tune and not from the spin oscillation amplitude and the fact that the depolarization is not significant for the first few hundred turns for any of the beam momentum spreads considered here.

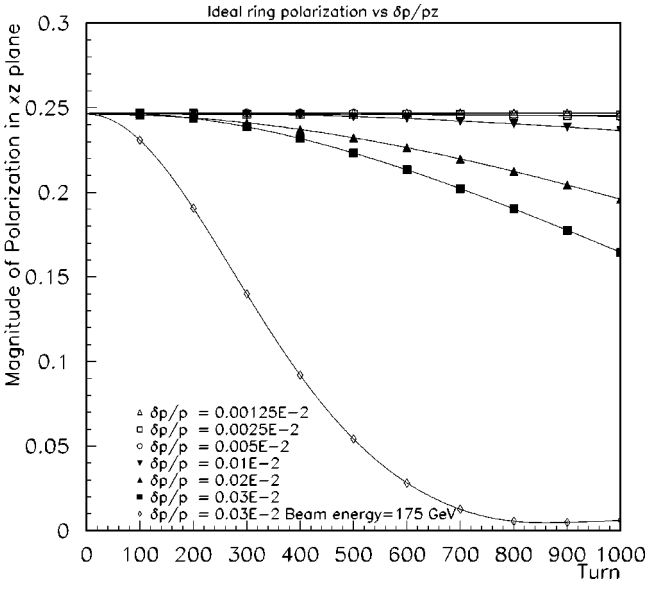

FIG. 13. Variation of polarization as a function of turn number for 50 GeV muons with initial $\hat{P}=-0.26$ and various values of $\delta p/p$ in an ideal collider ring. The bottom curve is for 175 GeV muons and shows a more rapid depolarization due to the higher spin tune.

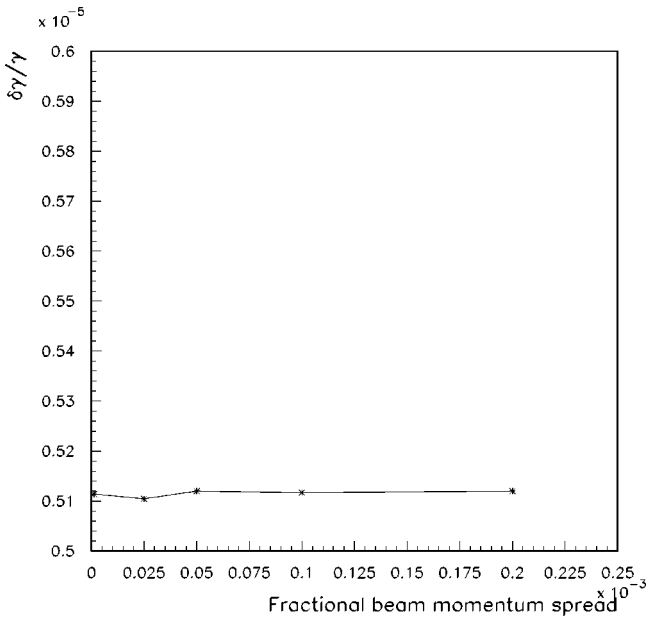

FIG. 14. $\delta\gamma/\gamma$ versus fractional beam energy spread for 50 GeV muons with PERR$=0.5\times10^{-2}$ and $\hat{P}=-0.26$.

C. Optimization of the electron energy cut

We now vary the cut on electron energy and study the dependence on $\delta\gamma/\gamma$ on the cut. Figure 15 shows the variation of $\delta\gamma/\gamma$ with the cut on individual electron energies for $\hat{P}=-0.26$ for 41 261 and 1146 electrons sampled. As shown in the Appendix, the fractional error on the average energy of electrons is much smaller than the fractional error on the total energy of electrons. It is possible to measure the average electron energy by counting the number of electrons going into the calorimeter with a scintillator array. However, the precession information is contained increasingly in the number of electrons rather than their average energy as we increase the electron energy cut. Figure 15 shows the variation of $\delta\gamma/\gamma$ calculated from the average as well as total electron energy as a function of the electron energy cut. For smaller values of the electron energy cut, the average method produces superior errors than the total energy method. However, with 40 000 electrons or more sampled a total energy method with a cut of 25 GeV or higher seems optimal. It should, however, be pointed out that the average energy method does not require a model for the rate of decay of muon intensity in the machine, which in practice could be a complicated function of turn number. As such the systematics associated with this would not be present in the average energy method. Figure 16(a) shows the variation of the absolute value of C/F as a function of the electron energy

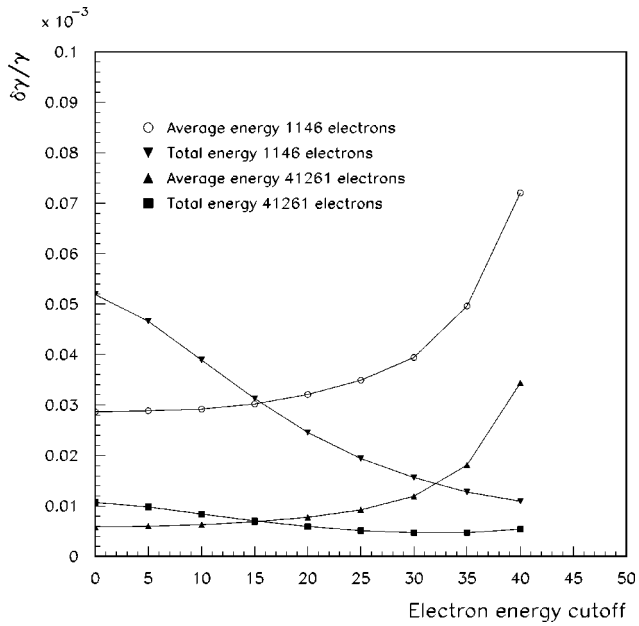

FIG. 15. The variation of $\delta\gamma/\gamma$ as a function of the electron energy cut for 41 261 and 1146 electrons, $\hat{P}=-0.26$. We fit the total energy in the calorimeter as well as the average energy per electron.

cutoff for $\hat{P}=-0.26$, where C and F are defined in Eq. (1.10) for both the total energy method and the average energy method. Figure 16(b) shows the fraction of electrons that lie above the electron energy cut as a function of the energy cut. The polarization for this sample is 0, since the electron energy fraction depends on polarization as well. Given the curves shown in Fig. 16, it should be possible to estimate the error in $\delta\gamma/\gamma$ for a variety of conditions.

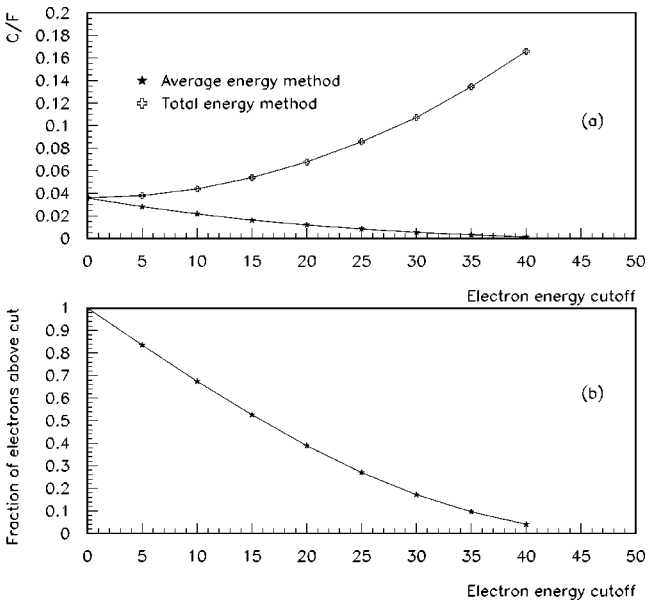

FIG. 16. (a) The variation of C/F as a function of the electron energy cut for $\hat{P}=-0.26$ for the total energy method and average energy method. (b) The fraction of electrons that survive the energy cut as a function of the cut for $\hat{P}=0$.

III. EFFECTS DUE TO DEPARTURES FROM THE IDEAL CASE

So far we have considered a planar collider ring with uniform vertical magnetic field and no electric fields. The actual collider ring will depart from the ideal in three respects: (a) It will have rf electric fields to keep the muons bunched, (b) it will have radial horizontal magnetic fields experienced by particles in an off-center trajectory at quadrupoles and at vertical correction dipoles, and (c) it will have longitudinal magnetic fields due to solenoidal magnets in the interaction region(s). We now consider the effect due to each of these departures from the ideal.

A. Electric fields

Equation (1.2) implies that there is no spin precession due to longitudinal electric fields ($\vec{\beta}\times\vec{E}=0$). rf electric fields are longitudinal, and so there will be no precession due to the rf electric fields. At present there are no plans to install electrostatic separators to separate the beams. If and when this happens, one should consider the effect due to the transverse electric fields thus introduced.

B. Effect of radial magnetic fields

Particles which are off axis at quadrupoles will experience radial as well as vertical magnetic fields. Even though the net integral of these off-axis fields around the ring is zero, the spin rotation along a horizontal axis followed by a spin rotation about a vertical axis (caused by a bend dipole) followed by a reverse rotation in the horizontal direction still produces a net effect since the rotations about the horizontal and vertical axes do not commute. The effects have been analyzed by Assmann and Koutchouk [5] who show that this results in both a net spin tune shift $\langle\delta\nu\rangle$ as well as a spread in tune $\sigma_{\delta\nu}$:

$$\langle\delta\nu\rangle=\frac{\cot\ \pi\nu_0}{8\pi}\nu_0^2[n_Q(Kl_Q)^2\sigma_y^2+n_{CV}\sigma_{\theta CV}^2], \quad (3.1)$$

where $\nu_0\equiv a\gamma$ is the spin tune of the collider ring, n_Q are the number of quadrupoles with integrated gradient Kl_Q, σ_y is the misalignment spread of the closed orbit at the quadrupoles, n_{CV} is the number of vertical correction dipoles, and $\sigma_{\theta CV}$ is the rms bend angle in the vertical correctors. The spread in tune is given by

$$\sigma_{\delta\nu}=\frac{\langle\delta\nu\rangle}{\cos\ \pi\nu_0}. \quad (3.2)$$

Table III shows the values for $\langle\delta\nu\rangle$ and $\sigma_{\delta\nu}$ obtained by Assman and Koutchuk [5] for the CERN e^+e^- collider LEP. We compare this with the current design for the 50 GeV muon collider ring [6]. Including the low beta section, there are 70 quadrupoles with an rms value of $Kl_Q=0.27\ \mathrm{m}^{-1}$. The effects due to correction dipoles may be neglected in both the LEP and the muon collider cases. We assume a beam misalignment of 5 mm at the quadrupoles, which is the same value used in the LEP calculation. This is probably

TABLE III. Predictions for spin tune shift $\delta\nu$ and spread in spin tune shift $\sigma_{\delta\nu}$ caused by quadrupoles for LEP compared to the 50 GeV muon collider ring.

Machine	Spin tune ν_0	Quadrupoles	rms Kl_Q (m^{-1})	σ_y (m)	$\delta\nu$	$\sigma_{\delta\nu}$
46 GeV LEP	100.47	≈600	0.032	0.5×10^{-3}	5.7×10^{-6} ≡3keV	6.1×10^{-5} ≡30 keV
50 GeV Muon Collider	0.5517	70	0.274	0.5×10^{-3}	-0.26×10^{-8} ≡−0.24 keV	1.66×10^{-8} ≡1.46 keV

being conservative. The tune shift for LEP corresponds to a shift in beam energy calibration of 3.0 keV. The tune spread for LEP corresponds to a spread in beam energy calibration of 30 keV. For the muon collider, the tune shift corresponds to a shift in beam energy calibration of -0.24 keV and a spread of 1.46 keV, both of which are negligible. The reason for the smallness of this effect for the muon collider is twofold. Since the circumference of the muon collider is smaller than LEP, there are fewer quadrupoles. Second, the muon is 200 times more massive than the electron and has a spin tune $a\gamma$ that is smaller by the same factor. The spin tune shift depends on the the square of the spin tune. It should be noted that the above formulas are not valid for a fractional spin tune of 0.5.

C. Solenoidal magnetic fields

The experimental region will in all likelihood contain a solenoidal magnet. This solenoidal field, if uncorrected, will rotate the spin vector of the muons about the beam direction by a constant amount θ_s per turn, which can be derived using Eq. (1.2):

$$\theta_s = -\frac{e}{\gamma m_\mu}(1+a)B_s = -(1+a)\frac{B_s l}{B\rho}, \tag{3.3}$$

where B_s is the field due to the solenoid of length l, and B and is the dipole bending field of the ring of radius ρ. For a solenoid of 1.5 T and length 6 m, $\theta_s = 3.09°$ for the planar storage ring parameters of Table I. It can be shown analytically [8] that this produces a spin tune shift $\delta\nu$ given by

$$\nu + \delta\nu = \frac{1}{\pi}\arccos\left[\cos(\pi\nu)\cos\left(\frac{\theta}{2}\right)\right], \tag{3.4}$$

yielding a spin tune shift $\delta\nu = -1.901\times10^{-5}$, or a fractional spin tune shift of $\delta\nu/\nu = -3.45\times10^{-5}$. For a 50 GeV muon beam, this is a shift in energy calibration of -1.72 MeV. In LEP, a similar solenoid will have a much smaller fractional tune shift [8], since the tune is 200 times larger for electrons. It is important to correct the effect due to the solenoids, since this is cumulative turn by turn. At LEP this is done by a series of vertical orbit correctors [9] followed by normal lattice followed by vertical orbit correctors of reverse polarity, which has the effect of rotating the spin by half the amount produced by the solenoid. A similar set of corrections is inserted after the solenoid to complete the correction. This method depends on a nonzero value of $g-2$ and as such will be 200 times less effective for muons than for electrons, for any given magnet strength. The most effective method to correct for the solenoid is to surround it on either side by compensating solenoids of minimal radius large enough to allow the beam to go through.

IV. POSSIBLE IMPLEMENTATION STRATEGY

We have given some thought to techniques to measure the energy due to decay electrons. Our current plans entail an electromagnetic calorimeter that is segmented both longitudinally and transversally placed inside an enlarged beam pipe in one of the straight sections in the collider ring. The length of the straight section upstream of the calorimeter can be chosen to control the number of decays (3.2×10^6 decays per meter for a beam intensity of 10^{12} muons) and hence the rate of energy deposition. The sensitive material can be gaseous, since the energy resolution is controlled by decay fluctuations rather than sampling error. In order to measure the total number of electrons entering the calorimeter, we plan to include a calorimeter layer with little absorber upstream of it as the first layer.

V. CONCLUSIONS

We have demonstrated that it is feasible to measure the energy of a 50 GeV muon collider to a few parts per 10^6 using the $g-2$ spin precession technique, provided it is feasible to maintain a muon polarization of the order of $\hat{P} = 0.25$ in the ring for 1000 turns. In order to explore the Higgs resonance, it is necessary to measure the bunch-by-bunch variation in energy to a few parts per 10^6. We have demonstrated that the $g-2$ technique is capable of doing so. It is still possible to tolerate a spin tune shift in the overall energy scale of a few percent, which will act only as a systematic error on the Higgs boson mass and width.

We would also like to note in passing that polarization information from a calorimeter of the type proposed here can be used in conjunction with a neutrino detector placed along the line of the neutrinos produced in association with the electrons to estimate the variation in the energy spectrum of the muon neutrinos and electron antineutrinos in the beam. Such information can be a valuable tool in untangling various possible neutrino oscillation scenarios.

We intend to develop the method here by studying the propagation of polarized muons in a realistic 50 GeV collider lattice using the program COSY [7], which takes into account nonlinear effects in the dynamic aperture. Design and Monte

Carlo studies will also be undertaken to develop the calorimeter detector needed.

ACKNOWLEDGMENTS

The authors would like to acknowledge useful conversations with Alain Blondel, Yaroslav Derbenev, and Robert Rossmanith.

APPENDIX

1. Treatment of errors

We measure the total energy E of all electrons with individual energy $e>25$ GeV in an electromagnetic calorimeter. Let N be the number of electrons sampled during a turn. N can fluctuate from sampling to sampling. Then

$$E=\sum_{i=1}^{N} e_i = N\langle e\rangle \tag{A1}$$

$$\frac{\sigma_E^2}{\langle E\rangle^2}=\frac{\sigma_N^2}{\langle N\rangle^2}+\frac{\sigma_{\langle e\rangle}^2}{\langle e\rangle^2}=\frac{1}{\langle N\rangle}\left(1+\frac{\sigma_e^2}{\langle e\rangle^2}\right), \tag{A2}$$

where the variance σ^2 of the quantities e and E results from the kinematic distributions of those quantities and not from the measurement errors. The average of the individual electron energies is denoted by $\langle e\rangle$.

Let the calorimeter be such that it measures the true deposited energy E with a resolution $\epsilon(E)$ such that

$$\frac{\epsilon^2}{E^2}=\mathcal{C}^2+\frac{\mathcal{S}^2}{E}+\frac{\mathcal{N}^2}{E^2}, \tag{A3}$$

where $\mathcal{C}$, $\mathcal{S}$, and $\mathcal{N}$ represent the constant, sampling, and noise terms, respectively. Let us assume that the measurement errors are Gaussian. Then,

$$P(E_m)=\int P(E)G(E,E_m,\epsilon)dE, \tag{A4}$$

where E_m is the measured energy and $G(E,E_m,\epsilon)$ is a Gaussian of mean E and standard deviation ϵ, which is a function of E and is written as $\epsilon(E)$. From this it follows that the mean measured energy $\langle E_m\rangle$ and the mean-squared measured energy $\langle E_m^2\rangle$ are given by

$$\begin{aligned}\langle E_m\rangle &= \int E_m P(E_m)dE_m \\ &= \int E_m dE_m \int P(E)G(E,E_m,\epsilon)dE \\ &= \int P(E)dE \int E_m G(E,E_m,\epsilon)dE_m \\ &= \int P(E)dE\times E = \langle E\rangle.\end{aligned} \tag{A5}$$

Equation (A5) states that the mean value of any distribution given by $P(E)$ is the same as that of the smeared distribution $P(E_m)$ provided the smearing function is such that the average of the smeared values for any given true value E equals the true value (a property satisfied by Gaussians) and the integration is carried over the full range of the variables. As an aside, in high energy physics, we measure steeply falling spectra that are smeared by measurement errors. Provided there is no arbitrary lower cutoff in the measured spectra (such as a trigger threshold), the above result would be valid, even for non-Gaussian resolutions. For the muon collider, the cutoff in selected electrons of 25 GeV is imposed by momentum selection that is independent of the calorimetry. So the above result would still be valid. Similarly, one can compute $\langle E_m^2\rangle$:

$$\begin{aligned}\langle E_m^2\rangle &= \int E_m^2 P(E_m)dE_m \\ &= \int E_m^2 dE_m \int P(E)G(E,E_m,\epsilon)dE \\ &= \int P(E)dE \int E_m^2 G(E,E_m,\epsilon)dE_m \\ &= \int P(E)dE\times(E^2+\epsilon^2) = \langle E^2\rangle + \int P(E)\epsilon^2(E)dE.\end{aligned} \tag{A6}$$

From this it follows that the variance of the measured energy, $\sigma_{E_m}^2$, is given by

$$\sigma_{E_m}^2=\sigma_E^2+\int P(E)\epsilon^2(E)dE \approx \sigma_E^2+\epsilon^2(\langle E\rangle), \tag{A7}$$

where the last approximation results from assigning the average measurement resolution to the resolution at the average energy. This then leads to

$$\frac{\sigma_{E_m}^2}{\langle E_m\rangle^2}\approx\frac{\sigma_E^2}{\langle E\rangle^2}+\frac{\epsilon^2(\langle E\rangle)}{\langle E\rangle^2}. \tag{A8}$$

Using Eqs. (A2) and (A3) leads to

$$\frac{\sigma_{E_m}^2}{\langle E_m\rangle^2}\approx\frac{1}{N}\left(1+\frac{\sigma_e^2}{\langle e\rangle^2}\right)+\mathcal{C}^2+\frac{\mathcal{S}^2}{N\langle e\rangle}+\frac{\mathcal{N}^2}{N^2\langle e\rangle^2}. \tag{A9}$$

From the above equation, it is obvious that the calorimeter must be such that the constant term $\mathcal{C}$ must be negligible for the fractional resolution to scale inversely with the number N of electrons collected. The noise term can be neglected for large enough N since it goes as N^{-2}. With these assumptions, one gets

$$\frac{\sigma_{E_m}^2}{\langle E_m\rangle^2}\approx\frac{1}{N}\left(1+\frac{\sigma_e^2}{\langle e\rangle^2}+\frac{\mathcal{S}^2}{\langle e\rangle}\right). \tag{A10}$$

For a 50 GeV muon beam, the values of $\langle e \rangle$ and σ_e are 34.05 GeV and 6.046 GeV, respectively, for electrons with $e > 25$ GeV. The ratio, $\sigma_e / \langle e \rangle$ is to a good approximation independent of muon energy. This then leads to the following error formula:

$$\frac{\sigma^2_{E_m}}{\langle E_m \rangle^2} \approx \frac{1}{N}\left(1 + 0.031\,53 + \frac{\mathcal{S}^2}{34.05}\right). \tag{A11}$$

Sampling terms of 0.15 $\mathrm{GeV}^{1/2}$ or better are easy to obtain in electromagnetic calorimeters. This leads to

$$\frac{\sigma^2_{E_m}}{\langle E_m \rangle^2} \approx \frac{1}{N}(1 + 0.031\,53 + 0.000\,661); \tag{A12}$$

i.e., the sampling term can be neglected when compared to the fluctuation in the true electron energies. So if the fractional measurement error $\mathrm{PERR} \equiv \sigma_{E_m} / \langle E_m \rangle$ is specified, the equivalent number of electrons is given by

$$N \approx \frac{1.031\,53}{(PERR^2)}. \tag{A13}$$

In other words, $\mathrm{PERR} = 0.5 \times 10^{-2}$, 1.0×10^{-2}, 2.0×10^{-2}, and 3.0×10^{-2} implies 41 261, 10 315, 2579, and 1146 electrons sampled. If in practice we sample 100 000 electrons, this leads to a value of $\mathrm{PERR} = 0.3212 \times 10^{-2}$. In order for this good a resolution to be meaningful, the constant term $\mathcal{C}$ has to be below this order of magnitude.

2. Using averages

Equation (A2) holds for the total energy E in the calorimeter. If, however, one also measures the total number of particles entering the calorimeter (using a scintillator system, for example, that counts minimum ionizing particles), then for each turn one can measure the average energy E_{av} of electrons. The fractional error on E_{av} does not contain a term due to the fluctuation of the number of electrons entering the calorimeter, being given by

$$\frac{\sigma^2_{E_{av}}}{\langle E_{av} \rangle^2} = \frac{\sigma^2_{\langle e \rangle}}{\langle e \rangle^2} = \frac{1}{\langle N \rangle}\left(\frac{\sigma^2_e}{\langle e \rangle^2}\right), \tag{A14}$$

with $\langle E_{av} \rangle = \langle e \rangle$. For a fractional error of PERR in E_{av}, the equivalent number of electrons sampled would be given by

$$N \approx \frac{0.031\,53}{(\mathrm{PERR}^2)}. \tag{A15}$$

With this method, $\mathrm{PERR} = 0.5 \times 10^{-2}$, 1.0×10^{-2}, 2.0×10^{-2}, and 3.0×10^{-2} implies 1261, 315, 79, and 35 electrons sampled, assuming no error in the measurement of N. If we sample 100 000 electrons, the fractional error in the average would be 0.561×10^{-3}. For this error to be meaningful, the sampling term would have to be of this order of magnitude.

[1] V. Bargmann, L. Michel, and V. L. Telegdi, Phys. Rev. Lett. **2**, 435 (1958).

[2] Particle Data Group, R. M. Barnett *et al.*, Phys. Rev. D **54**, 1 (1996).

[3] G. Barr, T. K. Gaisser, and T. Stanev, Phys. Rev. D **39**, 3532 (1989).

[4] F. James, CERNLIB computer program MINUIT.

[5] R. Assmann and J. P. Koutchouk, ''Spin tune shifts due to optics imperfections,'' CERN Report No. SL/94-13. See also L. Arnaudon *et al.*, Z. Phys. C **66**, 45 (1995).

[6] Carol Johnstone (private communication).

[7] M. Berz, COSY INFINITY version 7 user's guide and reference manual, Michigan State University Report No. MSUCL-977.

[8] J. P. Kouthcouk, ''Spin tune shift due to solenoids,'' CERN Report No. SL-note/93-26 (AP), 1993.

[9] R. Rossmanith, LEP Report No. 525, 1985; A. Blondel, LEP Report No. 629, 1990.